International Journal of Automotive Technology, Vol. 6, No. 6, pp. 635–641 (2005)

1229–9138/2005/024–11

ALUMINUM SPACE FRAME B.I.W. OPTIMIZATION CONSIDERING MULTIDISCIPLINARY DESIGN CONSTRAINTS

B. J. KIM[1)], M. S. KIM[2)] and S. J. HEO[2)*]

[1)]Vehicle CAE Team, Hyundai Motor Company, 772-1 Jangduk-dong, Whasung-si, Gyeonggi 445-706, Korea
[2)]School of Mechanical and Automotive Engineering, Kookmin University, Seoul 136-702, Korea

(Received 4 October 2004; Revised 29 October 2005)

ABSTRACT–This paper presents an ASF (Aluminum Space Frame) BIW (Body in White) optimal design, which minimizes weight and satisfies multidisciplinary constraints such as static stiffness, vibration characteristics, low-/high-speed crash, and occupant safety. As only one cycle CPU time for all the analyses is 12 hours, the ASF design having 11-design variable is a large scaled problem. In this study, ISCD-II and conservative least square fitting method were used for efficient RSM modeling. Likewise, the ALM method was used to solve the approximate optimization problem. The approximate optimum was sequentially added to remodel the RSM. The proposed optimization method uses only 20 analyses to solve the 11-design variable problem. Moreover, the optimal design can achieve 15.6% weight reduction while satisfying all the multidisciplinary design constraints.

KEY WORDS : ASF (Aluminum Space Frame), DOE (Design of Experiment), RSM (Response Surface Model), Multidisciplinary design constraints

1. INTRODUCTION

The application of alternative lightweight materials, development of new processing and assembly techniques, and design optimization technology can be considered at the initial development stage for body weight reduction. In particular, the development of the aluminum space frame (ASF) vehicle through the application of high-strength aluminum and manu-facturing technology can be cited as a representative example in connection with the selection of alternative lightweight materials. Unlike the conventional steel body, an aluminum body can generally realize more than 30% weight reduction while maintaining nearly equal stiffness. Since an aluminum body can increase the thickness of the ASF section, it can also help improve the performance of body NVH during engine idling as well as local strength and service life of the body (Gitter, 1990; Kang and Huh, 2000; Kim and Heo, 2003; Kim *et al.*, 2002; Roger and Scatt, 2000).

Designing a body considering all these features of high strength aluminum requires satisfying multidiscip-linary design constraints such as bending and torsion stiffness, vibration characteristics, crashworthiness of the vehicle, and less weight at the initial design stage. Since considering these multidisciplinary design constraints is very complicated and difficult, however, the design method that derives the optimum design schemes in the respective fields and allows trade-off between the disciplines has been applied to date. Still, consolidating the conflicting design schemes of these design values require considerable time and cost.

This paper proposes a design method that considers the multidisciplinary design constraints (Sobieszczanski *et al.*, 2000; Yang *et al.*, 2000) for the initial stage design of an ASF body. Design considerations included static stiffness, vibration characteristics, low-/high-speed crash, and occupant safety. All 11 thicknesses in the ASF section were selected as design variables. The ISCD-II (Incomplete Small Composite Design-II) DOE table was applied to the minimum analysis. Likewise, the SVD (Singular Value Decomposition) based least square method was utilized to overcome the singular phenomena due to the fewer experimental points than the unknown of the RSM model. Finally, for more refined design, the sequential approximate optimization combined with RSM models was carried out using the ALM (Augmented Lagrange Multiplier) technique (Kim, 2001; Kim and Heo, 2003; Kim, 2004).

2. ANALYSIS OF THE ASF BASE MODEL BY FIELD

The analysis of the ASF base model was carried out

*Corresponding author. e-mail: sjheo@kookmin.ac.kr

preferentially, considering the multidisciplinary constrained design optimization.

2.1. Analysis of Static Stiffness

The stiffness of a body is generally an evaluation of deformation in a bent or twisted body as illustrated in Figure 1. Bending stiffness is evaluated by appropriately constraining the degree of freedom at 4 points of the suspension combination part and applying load to the center of the car. On the other hand, for torsion stiffness, the torsion deformation of a body is evaluated by fixing the combination part of the rear suspension and applying torsion load to opposite directions on the combination part of the front suspension.

The evaluation and analysis of static stiffness used MSC/NASTRAN. The finite elements of the model consisted of 54,791 shell elements. Using Pentium IV 2.8 GHz CPU, analysis took 167 seconds. Figure 2 shows the deformed shapes. In this study, the maximum displacement value was considered in design constraints. The maximum bending displacement of the ASF base model was 0.255 mm, and the maximum torsion displacement, 1.289 mm.

2.2. Modal Analysis

In designing a body structure, the vibration characteristics of a body should be considered in connection with static stiffness. When the body stiffness is too low, the body stiffness should be improved since body can crack or noise and vibration problems are occurred. The modal

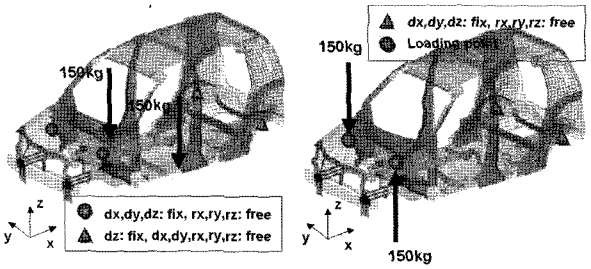

(a) Bending stiffness analysis (b) Torsion stiffness analysis

Figure 1. Load and boundary conditions for the static stiffness analysis of the ASF base model.

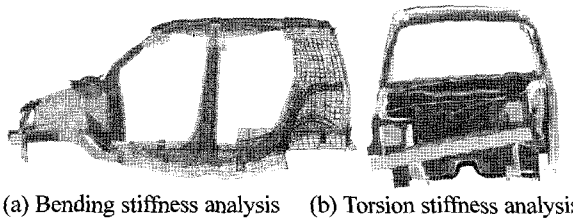

(a) Bending stiffness analysis (b) Torsion stiffness analysis

Figure 2. Results of the static stiffness analysis of the ASF base model.

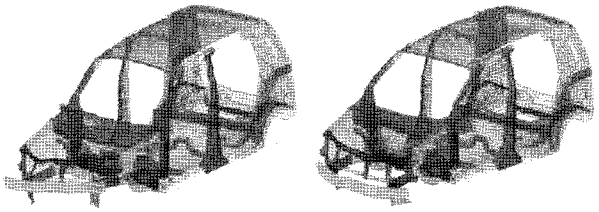

Figure 3. Results of the normal mode analysis of the ASF base model.

analysis was carried out to examine the characteristic number of vibrations and mode shape of the ASF base model. The ASF BIW model was the same as the model used in the analysis of static stiffness, with the calculation of MSC/NASTRAN taking 1047 seconds. Figure 3 shows the first mode of torsion and bending.

2.3. Crash Analysis

During vehicle design, crash is one of the most important design fields that should be considered. It is divided into the low-speed and high-speed crash design concepts. The high-speed crash design concept is a key to maximizing the absorbed crash energy and lowering the value of occupant injury through axial-direction deformation or bending deformation in colliding structural members. On the other hand, the low-speed crash design concept seeks to reduce the possibility of damage and repairs by preventing the deformation of major colliding structural members as much as possible. Therefore, a more efficient crash design can be realized when two conflicting design concepts are both considered. In this paper, the FMVSS 208 test certification standard was applied as the high-speed crash constraint, and CMVSS 215, a Canadian bumper crash absorption test certification standard, as the low-speed crash constraint.

2.3.1. Analysis of high-speed crash

To analyze the crash characteristics of the ASF base model, crash analysis was conducted by applying the FMVSS 208 test certification standard. The finite element of the ASF base model used consisted of 93,389 shell elements and 1,435 beam elements. Analysis using PAM-CRASH took 7 hours and 30 minutes in a Pentium IV 2.8 GHz CPU. Figure 4 indicates the initial crash speed and boundary conditions following the FMVSS 208 certification test. The analysis end time was set as 80 msec. Reviewing the analysis result as shown in Figure 5 revealed a structure that absorbs crash energy with the axial-direction collapse of the front side member and bending deformation of the sub-frame. Since the total crash energy was 52603J, and the energy absorbed by the side member, 17382J, the side member was confirmed to

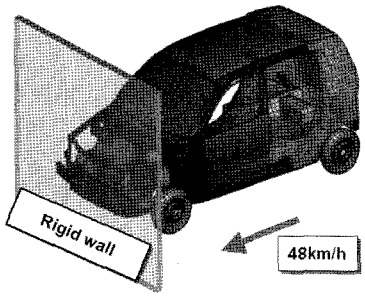

Figure 4. Initial velocity and boundary condition.

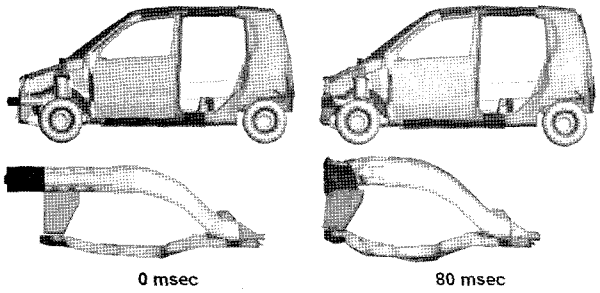

Figure 5. Results of the high-speed crash analysis.

have absorbed about 33% of the entire crash energy.

2.3.2. Analysis of occupant behavior

For the occupant safety analysis of the ASF base model, PAM-CRASH was used. In the B-pillar lower end, the acceleration data derived from the high-speed crash analysis was inputted into the sled model. Analysis took about 501 seconds in Pentium IV 2.8 GHz CPU.

Figure 6 shows the analysis results, which depict occupant behavior. The acceleration data of the dummy's head and chest is shown in Figure 7. Following the extracted acceleration-time waveform and using Equation (1), the HIC value, i.e., extent of injury of the dummy's head, was calculated to be 464.69. The maximum acceleration of the chest part was expressed as the ratio against

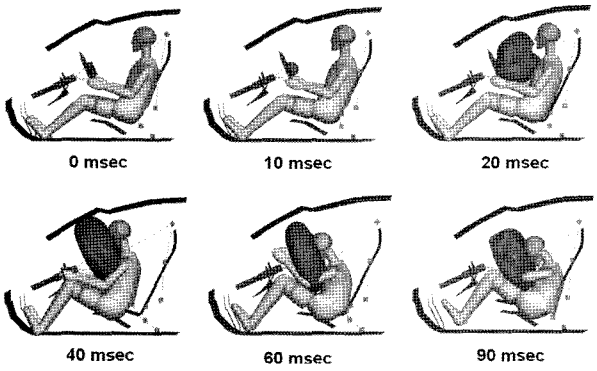

Figure 6. Occupant behavior during the sled analysis.

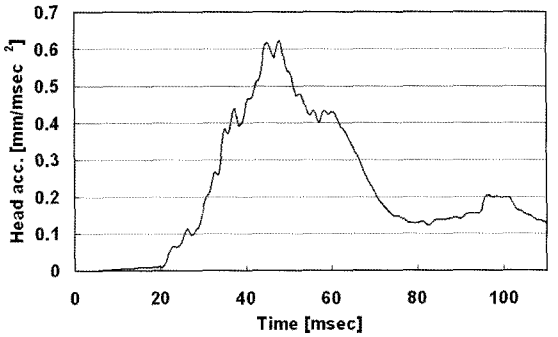

(a) Head acceleration

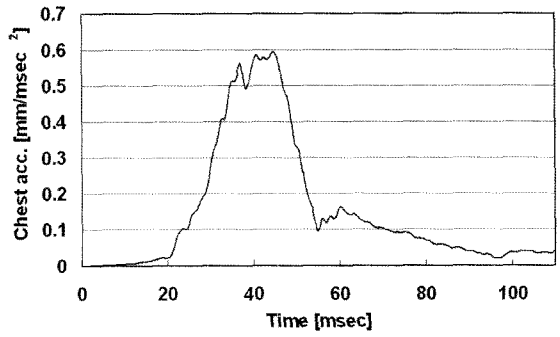

(b) Chest acceleration

Figure 7. Head and chest acceleration results.

gravitational acceleration during 3 msec (58.95 g). These results indicated that all the limit values of the injury suggested in FMVSS 208 were satisfied.

$$HIC = \max_{t_2 < t_1} \left[\left\{ \frac{1}{t_2 - t_1} \int_{t_1}^{t_2} a(t)dt \right\}^{2.5} (t_2 - t_1) \right] \quad (1)$$

Figure 8. Bumper back beam deformation behavior during the low-speed crash analysis.

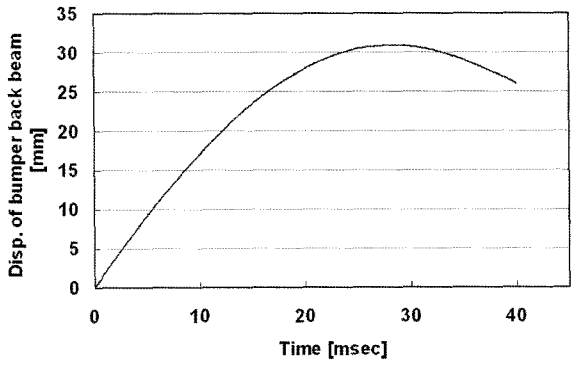

Figure 9. Bumper back beam displacement.

2.3.3. Analysis of low-speed crash

The low-speed crash analysis of the ASF base model at 5MPH and fixed wall was conducted using PAM-CRASH as per the CMVSS 215 regulation. Analysis took about 3 hours and 6 minutes in Pentium IV 2.8 GHz CPU. Figures 8 and 9 show the deformation behavior and displacement-time curve, respectively, of the bumper back beam. The maximum bumper deformation displacement was 30.9 mm.

3. OPTIMUM DESIGN OF THE ASF BIW MODEL CONSIDERING THE MULTI-DISCIPLINARY CONSTRAINTS

3.1. Selection of Design Variables and Objective Function

The optimum design of the ASF BIW was carried out considering the multidisciplinary constraints reviewed in the previous section. First, 11 design variables were selected uniformly over the entire structure of the ASF BIW as shown in Figure 10. All design variables consisted of the thicknesses of aluminum extruded materials except the B-pillar thickness of the structural member. The designations and upper/lower limit values of the respective design variables are listed in Table 1. Optimization aims to minimize the weight sum of the selected design variables.

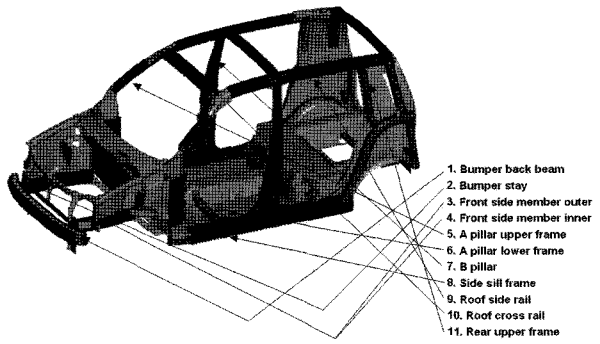

Figure 10. Design variables for ASF BIW optimization.

Table 1. Design variables and their limits.

Design variable	Component name	Lower value [mm]	Middle value [mm]	Upper value [mm]
DV1	Bumper back beam	1.0	1.5	2.0
DV2	Bumper stay	1.0	1.5	2.0
DV3	FR/SM outer	1.0	1.5	2.0
DV4	FR/SM inner	1.0	1.5	2.0
DV5	A pillar upper	2.0	2.5	3.0
DV6	A pillar lower	2.0	2.5	3.0
DV7	B pillar	5.0	6.0	7.0
DV8	Side-sill	2	3	4
DV9	Roof side rail	2	3	4
DV10	Roof cross member	2	2.5	3
DV11	Qtr upper	1	2	3

3.2. Analysis of Design Sensitivity

To evaluate the sensitivity of design variables for objective function and constraints, ISCD-II DOE table is generated as Table 2 and its corresponding analysis results are listed in Table 3. Only the representative sensitivity result for torsion displacement and crash energy was shown in Figure 11. The remainder design variables were found to exhibit either an upward or downward concave shape, except the No. 2, 6, 8 design variable for torsion displacement and No. 1 design

Table 2. ISCD-II DOE table.

	DV1	DV2	DV3	DV4	DV5	DV6	DV7	DV8	DV9	DV10	DV11
Model 1	2	2	1	2	3	3	5	2	2	3	1
Model 2	1	2	2	1	3	3	7	2	2	2	3
Model 3	2	1	2	2	2	3	7	4	2	2	1
Model 4	1	2	1	2	3	2	7	4	4	2	1
Model 5	1	1	2	1	3	3	5	4	4	3	1
Model 6	1	1	1	2	2	3	7	2	4	3	3
Model 7	2	1	1	1	3	2	7	4	2	3	3
Model 8	2	2	1	1	2	3	5	4	4	2	3
Model 9	2	2	2	1	2	2	7	2	4	3	1
Model 10	1	2	2	2	2	2	5	4	2	3	3
Model 11	2	1	2	2	3	2	5	2	4	2	3
Model 12	1	1	1	1	2	2	5	2	2	2	1
Base design	1.5	1.5	1.5	1.5	2.5	2.5	6	3	3	2.5	2

Table 3. Analysis results corresponding DOE table.

	Bend. disp. [mm]	Torsi. disp. [mm]	1st rotsi. freq. [Hz]	Crash energy [J]	HIC	Chest acc. [g]	Bump. disp. [mm]	Mass [kg]
Model 1	0.317	1.251	27.49	18519.47	458.08	57.95	21.35	40.08
Model 2	0.306	1.243	28.85	16967.81	476.96	60.03	47.73	44.18
Model 3	0.223	1.253	22.91	17630.02	502.03	61.65	32.52	50.99
Model 4	0.221	1.307	28.6	16865.71	460.83	59.66	48.65	52.91
Model 5	0.218	1.254	28.27	16562.65	586.78	61.58	48.25	50.61
Model 6	0.288	1.291	27.83	16096.37	468.26	62.26	47.55	49.49
Model 7	0.229	1.359	22.32	16069.76	464.17	58.87	30.71	53.63
Model 8	0.219	1.21	27.9	17283.47	451.39	57.79	22.28	51.58
Model 9	0.3	1.338	25.93	17968.92	522.21	60.78	20.67	48.64
Model 10	0.239	1.336	27.61	13972.03	445.11	59.95	48.36	47.07
Model 11	0.306	1.393	22.32	16903.45	473.68	59.96	32.64	43.89
Model 12	0.332	1.431	26.6	14904.59	468.15	60.92	46.42	34.95
Base design	0.255	1.289	27.6	17382.7	464.69	58.95	30.9	47.34

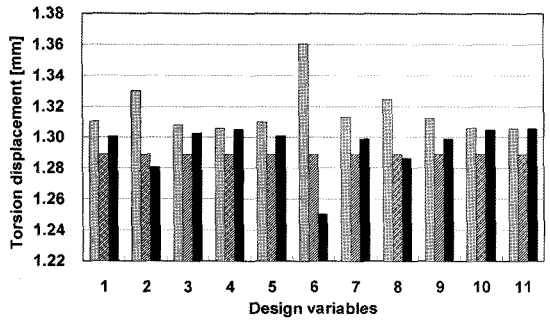

(a) Torsion displacement

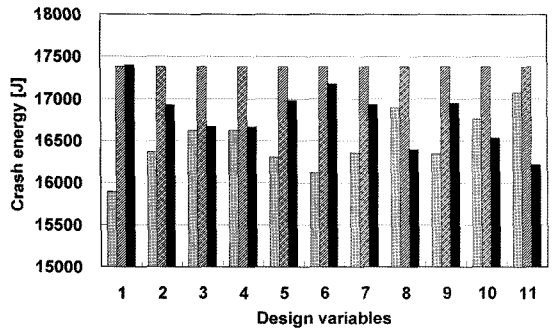

(b) Crash energy

Figure 11. Design sensitivity results for typical design constraints.

variable for crash energy. Moreover, it was very difficult to obtain optimum design points from the bar chart considering all these items. Therefore, approxi-mate optimization procedure using these factors should be performed.

3.3. Sequential Approximate Optimization

Based on the response surface model, optimum design was carried out considering the multidisciplinary constraints of the ASF BIW. Multidisciplinary constraints for optimization were set up, taking into account the analysis results in the respective fields of the ASF base model. Equations (2)–(10) represents the optimization formula for multidisciplinary constraints, considering the body stiffness, vibration, low-/high-speed crash, and occupant safety of the ASF BIW.

The abovementioned optimization problem was solved using R-INOPL (Kim and Huh, 2003). For the R-INOPL, the SVD technique was applied to solve the least square method with fewer experimental points compared to the number of the unknown. Moreover, to enhance the feasibility of the approximate optimum values, the conservative least square method (Kim and Huh, 2003), which generates approximate functions conservatively in accordance with the user's objective, was applied. The approximated optimization problem internally solved by using B-INOPL (Kim, 2001) based on the Augmented Lagrange Multiplier technique. In this study, the response surface model of the second order full quadratic was applied. Among multidisciplinary constr-aints, static bending displacement, torsion displacement, HIC, chest acceleration, and displacement of the bumper back beam were constructed by the over-estimate (Kim and Huh, 2003) model. Likewise, crash energy was generated using the under-estimate (Kim and Huh, 2003) model. Figure 12 shows the process that R-INOPL solves multidisciplinary constrained optimization problems. First, basic analysis results for DOE table are inputted to R-INOPL. Then, it gives a new approximated optimum.

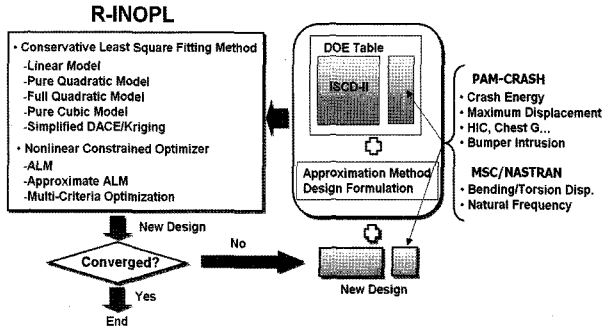

Figure 12. Sequential Approximate Optimization (SAO) process using R-INOPL.

New analyses are performed for this new design. These new results are added to the original DOE Table. R-INOPL is then performed again for the added DOE table and repeated until all constraints are converged. The updated response surface model can represent a more exact approximate solution through this process.

This study satisfied all design constraints only using the SAO process 7 times, with the results listed in Table 4 and Table 5. Figure 13 shows the convergence history of objective function and constraints. Constraints were then expressed with values normalized with the respective permissible values. Finally, Table 6 compares the ASF base model and the final model. Results showed about

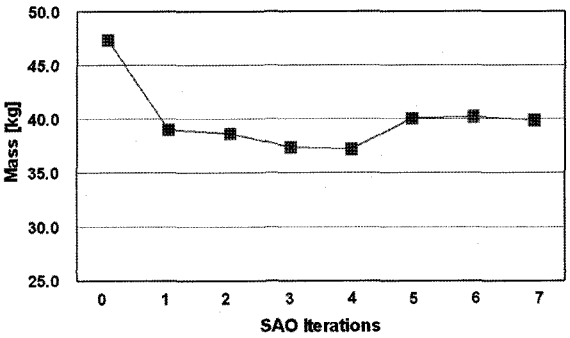

(a) Objective function

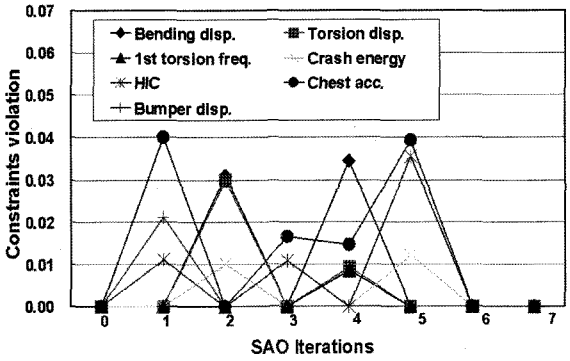

(b) Constraints violation

Figure 13. Convergence history of ASF BIW design optimization.

Table 4. Convergence history for design variables.

	DV1	DV2	DV3	DV4	DV5	DV6	DV7	DV8	DV9	DV10	DV11
Base design	1.5	1.5	1.5	1.5	2.5	2.5	6	3	3	2.5	2
SAO 1	1.370	1.574	1.294	1.207	2.033	3.000	5.000	2.482	2.000	2.000	1.448
SAO 2	1.418	1.797	1.000	1.270	2.378	2.236	5.000	2.421	2.038	2.000	1.831
SAO 3	1.434	2.000	1.027	1.221	2.243	2.570	5.000	2.609	2.010	2.000	2.072
SAO 4	1.725	2.000	1.000	1.325	2.150	2.396	5.000	2.360	2.038	2.000	2.379
SAO 5	1.481	2.000	1.001	1.176	2.452	2.451	5.000	2.568	2.107	2.077	2.052
SAO 6	1.363	2.000	1.000	2.000	2.416	2.478	5.226	2.534	2.065	2.079	1.881
SAO 7	1.412	2.000	1.000	1.870	2.212	2.405	5.024	2.634	2.000	2.002	1.888

Table 5. Convergence history for performance indexes.

	Bend. disp. [mm]	Torsi. disp. [mm]	1st rotsi. freq. [Hz]	Crash energy [J]	HIC	Chest acc. [g]	Bump. disp. [mm]	Mass [kg]
Base design	0.255	1.289	27.60	17382.70	464.69	58.95	30.90	47.34
SAO 1	0.289	1.269	27.85	17419.60	485.30	62.40	33.70	39.03
SAO 2	0.299	1.339	27.15	16828.15	461.82	59.42	30.65	38.66
SAO 3	0.286	1.287	28.00	17017.84	485.21	60.99	30.64	37.38
SAO 4	0.300	1.312	26.77	17337.90	460.95	60.88	26.85	37.21
SAO 5	0.288	1.300	27.73	16793.43	497.04	62.36	29.85	40.08
SAO 6	0.289	1.293	27.700	17021.16	471.22	59.35	32.15	40.23
SAO 7	0.288	1.299	27.550	17063.21	471.13	59.89	32.35	39.92

Table 6. Comparison of the initial and final designs.

System	Attribute	Baseline	Target	Final design result
Static stiffness	Bending disp. [mm]	0.255	≤0.29	0.288
	Torsion disp. [mm]	1.289	≤1.3	1.299
Vibr-ation	1st torsion mode frequ. [Hz]	27.6	$27 \le f_1 \le 28$	27.55
Low speed crash	Bumper disp. [mm]	30.9	≤35	32.55
High speed crash	Crash energy [J}	17382.7	≥17000	17063.21
	HIC	464.69	≤480	471.13
	Chest acc. [g]	58.95	≤60	59.89
	Mass [kg]	47.34	Minimize	39.92

15.6% weight reduction compared with the initial basic model, at the same time satisfying all multidisciplinary constraints.

$$\textit{Minimize mass}(T) \tag{2}$$

Subject to

$$\textit{Static bending displacement}(T)_{max} \le 0.29 \textit{ mm} \tag{3}$$

$$\textit{Static torsional displacement}(T)_{max} \le 1.3 \textit{ mm} \tag{4}$$

$$27\textit{Hz} \le \textit{Mode 1, Frequency}(T) \le 28 \textit{ Hz} \tag{5}$$

$$\textit{Crash energy}(T)_{min} \ge 17000\textit{J} \tag{6}$$

$$\textit{HIC}(T)_{max} \le 480 \tag{7}$$

$$\textit{Chest acc.}(T)_{max} \le 60g \tag{8}$$

$$\textit{Bumper displacement}(T)_{max} \le 35 \textit{ mm} \tag{9}$$

$$T_i^L \le T_i \le T_i^U, \ (i=1,2,\ldots 10,11) \tag{10}$$

4. CONCLUSION

In this study, body weight reduction design was carried out considering multidisciplinary constraints such as the static stiffness for bending and torsion, vibration characteristics for 1st bending and torsional natural frequencies, low-/high-speed crash performance, and occupant safety. Specifically, the response surface model for the respective performance indices was approximated using the ISCD-II DOE tables for minimizing fundamental analyses. Then, Sequential approximate optimization (SAO) was employed for solving this design problem. Using the proposed SAO method, 15.6% weight reduction was realized compared to the base model wherein analysis was carried out 20 times for the ASF body optimization design considering 11 design variables.

ACKNOWLEDGEMENT–This work was supported by research program 2005 of Kookmin-University in Korea. The authors gratefully acknowledge the financial support for research.

REFERENCES

Gitter, R. (1990). Designing with extruded aluminum sections. *Tagungsband DVM-Tag,* Berlin.

Kang, W. J. and Huh, H. (2000). Crash analysis of auto-body structures considering the strain-rate hardening effect. *Int. J. Automotive Technology* **1, 1,** 35–41.

Kim, B. J. and Heo, S. J. (2003). Collapse charac-teristics of aluminum extrusions filled with the structural foam for space frame vehicles. *Int. J. Automotive Technology* **4, 3,** 141–147.

Kim, H. Y., Kim, J. K., Heo, S. J. and Kang, H. (2002). Design of the impact energy absorbing members and evaluation of the crashworthiness of aluminum intensive vehicles. *Trans. Korean Society of Automotive Engineers* **10, 1,** 216–233.

Kim, M. S. (2001). B-INOPL Ver. 3.0: User's guide to the general constrained nonlinear optimization program.

Kim, M. S. and Heo, S. J. (2003). Conservative quadratic RSM combined with incomplete small composite design and conservative least square fitting. *KSME Int. J.* **17, 5,** 705–714.

Kim, M. S. (2004). User's guide to sequential approximate optimization program based on response surface models. R-INOPL Ver. 1.5.

Roger, W. L. and Scott, A. P. (1995). Energy absor-ption in aluminum extrusions for a space frame chassis. *SAE Paper No.* 951079.

Sobieszczanski-Sobieski, J., Kodiyalam, S. and Yang, R. J. (2000). Optimization of a car body under NVH (noise, vibration, and harshness) constraints and crash. *AIAA/ASME/AHS/ASC 41st Structures, Structural Dyn-amics, and Materials Conf., AIAA Paper No.* 2000-1521, Atlanta.

Yang, R. J., Gu, L., Tho, C. H. and Sobieszczanski-Sobieski, J. (2001). Multidisciplinary design optimization of a full vehicle through high-performance computing. *AIAA/ASME/AHS/ASC 42nd Structures, Structural Dynamics, and Materials Conf., AIAA Paper No.* 2001–1273, Seattle, Washington.